



HAL
open science

Constraining the high-redshift formation of black hole seeds in nuclear star clusters with gas inflows

A. Lupi, M. Colpi, B. Devecchi, G. Galanti, M. Volonteri

► **To cite this version:**

A. Lupi, M. Colpi, B. Devecchi, G. Galanti, M. Volonteri. Constraining the high-redshift formation of black hole seeds in nuclear star clusters with gas inflows. *Monthly Notices of the Royal Astronomical Society*, 2014, 442, pp.3616-3626. 10.1093/mnras/stu1120 . insu-03645336

HAL Id: insu-03645336

<https://insu.hal.science/insu-03645336>

Submitted on 25 Apr 2022

HAL is a multi-disciplinary open access archive for the deposit and dissemination of scientific research documents, whether they are published or not. The documents may come from teaching and research institutions in France or abroad, or from public or private research centers.

L'archive ouverte pluridisciplinaire **HAL**, est destinée au dépôt et à la diffusion de documents scientifiques de niveau recherche, publiés ou non, émanant des établissements d'enseignement et de recherche français ou étrangers, des laboratoires publics ou privés.

Constraining the high-redshift formation of black hole seeds in nuclear star clusters with gas inflows

A. Lupi,^{1★} M. Colpi,² B. Devecchi,³ G. Galanti¹ and M. Volonteri⁴

¹*DiSAT, Università degli Studi dell'Insubria, Via Valleggio 11, I-22100 Como, Italy*

²*INFN, Milano Bicocca, Piazza della Scienza 3, I-20126 Milano, Italy*

³*TNO, Electronic Defence*

⁴*Institut d'Astrophysique de Paris, 98bis Bd. Arago, 75014 Paris, France*

Accepted 2014 June 4. Received 2014 May 26; in original form 2014 January 10

ABSTRACT

In this paper, we explore a possible route of black hole seed formation that appeals to a model by Davies, Miller & Bellovary who considered the case of the dynamical collapse of a dense cluster of stellar black holes subjected to an inflow of gas. Here, we explore this case in a broad cosmological context. The working hypotheses are that (i) nuclear star clusters form at high redshifts in pre-galactic discs hosted in dark matter haloes, providing a suitable environment for the formation of stellar black holes in their cores, (ii) major central inflows of gas occur on to these clusters due to instabilities seeded in the growing discs and/or to mergers with other gas-rich haloes and (iii) following the inflow, stellar black holes in the core avoid ejection due to the steepening to the potential well, leading to core collapse and the formation of a massive seed of $\lesssim 1000 M_{\odot}$. We simulate a cosmological box tracing the build-up of the dark matter haloes and their embedded baryons, and explore cluster evolution with a semi-analytical model. We show that this route is feasible, peaks at redshifts $z \lesssim 10$ and occurs in concomitance with the formation of seeds from other channels. The channel is competitive relative to others, and is independent of the metal content of the parent cluster. This mechanism of gas-driven core collapse requires inflows with masses at least 10 times larger than the mass of the parent star cluster, occurring on time-scales shorter than the evaporation/ejection time of the stellar black holes from the core. In this respect, the results provide upper limit to the frequency of this process.

Key words: black hole physics – galaxies: evolution – galaxies: formation – galaxies: star clusters: general.

1 INTRODUCTION

Observations of high-redshift quasars show that black holes as massive as $\gtrsim 10^9 M_{\odot}$ were already in place at redshift $z \lesssim 7$ (Mortlock et al. 2011) when the Universe was only eight hundred million years old. It is thus challenging to understand how these black holes formed when the Universe was less than 1 Gyr old and galaxies were in the process of forming.

Current models suggest that supermassive black holes may have formed from *seeds* of yet unknown mass which later grew via sustained accretion at critical or supercritical rates, and via mergers with other black holes during the hierarchical assembly of their host haloes (Volonteri 2010). The origin and nature of this seed population(s) remain uncertain as uncertain are the physical mech-

anisms at play. This has led to speculate that black hole seeds had masses in a wide range, between 100 and $10^6 M_{\odot}$. To ensure early formation, seed black holes must have formed in the most massive and rare haloes of a given epoch which virialize and grow in the knots of the cosmic web (Di Matteo et al. 2008).

Seed black holes may have formed as early as redshift $z \sim 20$, from the core collapse of the first very massive stars ($\gtrsim 260 M_{\odot}$) formed out of pristine gas clouds fragmenting in virialized pre-galactic haloes of $10^{5-6} M_{\odot}$, i.e. the Pop III stars (Haiman, Thoul & Loeb 1996; Tegmark et al. 1997; Madau & Rees 2001; Heger et al. 2003). The lack of metals suggest a top-heavy initial mass function and thus a first generation of seed black holes of stellar origin with masses $\lesssim 10^3 M_{\odot}$ (Omukai & Palla 2001; Abel, Bryan & Norman 2002; Bromm, Coppi & Larson 2002; Bromm & Loeb 2003; Yoshida, Omukai & Hernquist 2008). But, recent studies seem to revise the initial estimates of the stellar masses to possibly much lower values of just a few tens of solar masses (Clark et al. 2011; Greif et al. 2011; Wise et al. 2012).

★ E-mail: alessandro.lupi@uninsubria.it

Heavy seeds can form at later times ($z \lesssim 12$) from the central collapse of gas in unstable proto-galactic discs of $10^{5-6} M_{\odot}$ present in heavier ($10^{7-8} M_{\odot}$) dark matter haloes (Koushiappas, Bullock & Dekel 2004; Begelman, Volonteri & Rees 2006; Lodato & Natarajan 2006). If the angular momentum barrier and the process of fragmentation are suppressed in some of these pre-galactic structures, due to e.g. the presence of a background of UV radiation (Agarwal et al. 2012; Latif et al. 2013), the infall of gas can continue unimpeded leading to the formation of seed black holes by direct collapse. Alternatively, a non-thermally relaxed giant star can form in these haloes which is able to grow a black hole (of $\lesssim 10 M_{\odot}$) in its centre (Begelman 2010; Choi, Shlosman & Begelman 2013). In this last case, subsequent super-Eddington growth of this embryo black hole continues, inside the optically thick hydrostatic envelope, called ‘quasi-star’ (Begelman, Rossi & Armitage 2008; Schleicher et al. 2013). Seed black holes as heavy as $10^{4-5} M_{\odot}$ can form, depending on the extent of the radiative feedback and metal content (Dotan, Rossi & Shaviv 2011; Montero, Janka & Müller 2012). A further path of black hole seed formation, not constrained by the limits imposed by the metallicity content, calls for gas-rich galaxy mergers which trigger huge inflows of gas on sub-parsec scales (Mayer et al. 2010). But avoiding fragmentation of the growing gas cloud due to cooling is again a matter of debate (Ferrara, Haardt & Salvaterra 2013).

An alternate route for seed formation (up to 10^2 – $10^3 M_{\odot}$) has been explored considering galactic discs enriched above a critical metallicity ($Z_{\text{crit}} \sim 10^{-5} Z_{\odot}$) and in which cloud fragmentation leads to ordinary Pop II star formation (SF; Devecchi & Volonteri 2009, D09 hereon). This path considers the formation, in some haloes, of a young ultradense nuclear star cluster (NSC hereafter) dominated by stellar collisions and mass segregation in its centre. A very massive star forms via star–star runaway collisions in the cluster core before single stars have time to explode in supernovae (SNe). The ensuing collapse of the runaway star eventually leads to the formation of a black hole above $\gtrsim 10^{2-3} M_{\odot}$ (Portegies Zwart & McMillan 2002; Gürkan, Freitag & Rasio 2004; D09).¹ In a cosmological context, this route has been explored by D09 who considered seed formation in pre-galactic discs. It was shown that NSCs of $10^{5-6} M_{\odot}$ develop as early as $z \sim 15$ – 10 and that the first seed black holes, from runaway stars, start dominating, below these redshifts, over the Pop III channel active at earlier epochs (D09, Devecchi et al. 2010, 2012, D10, D12 hereon, respectively).

1.1 The gas-induced runaway merger model: GIRM

None of the above-mentioned mechanisms consider the formation of massive black hole seeds from the runaway merger of *stellar* black holes in ultradense star clusters. This channel was studied by Quinlan & Shapiro in the late 1980s and has been revisited recently by Davies, Miller & Bellovary (2011) who introduced a variant to this model.

In Quinlan & Shapiro (1987), a very massive Newtonian cluster of compact stars (neutron stars and stellar black holes) evolves dynamically into a state of catastrophic core collapse. Under the rather extreme conditions considered by Quinlan & Shapiro (i.e.

of a galactic nucleus of 10^{7-8} stars with high initial velocity dispersion $\gtrsim 1000 \text{ km s}^{-1}$), binaries of compact stars form mainly via dissipative two-body encounters under the control of gravitational wave emission, ending in their coalescence. Following unimpeded self-similar core collapse, the central density, gravitational potential and velocity dispersion rise up to a critical limit corresponding to the onset of a relativistic dynamical instability (when the gravitational redshift z_{grav} rises above ~ 0.5). A central $\gtrsim 100 M_{\odot}$ black hole forms embracing the mass of the collapsing core.

In a subsequent paper, Quinlan & Shapiro (1989) recognized that the inclusion of a realistic mass spectrum for the compact stars combined with an accurate modelling of the stellar dynamics prevents the core from reaching the high-velocity dispersions requested for the onset of the relativistic dynamical collapse. Fast mass segregation by dynamical friction combined with the tendency of stars to reach equipartition of kinetic energy (i.e. lower dispersion velocities for the heavier stars) led the core to evolve into a state of declining velocity dispersion, preventing the deepening of the gravitational potential well with time up to $z_{\text{grav}} \sim 0.5$ (see e.g. fig. 3 of Quinlan & Shapiro 1989). The ultimate fate of the stellar black holes left in the centre was then found very difficult to calculate and predict, within the limits imposed by the Fokker–Planck approximation used to study the system.²

Quinlan & Shapiro (1987) first recognized that only in massive galactic nuclei of 10^{7-8} stars with velocity dispersions in excess of 1000 km s^{-1} , binary stars, known to act as a kinetic energy source, do not heat dynamically the cluster to halt and reverse the gravothermal catastrophe of the core. In lower mass systems, such as globular clusters comprising 10^{5-6} stars, recent numerical studies indicate that most of the stellar black holes born from ordinary stellar evolution, either single or in binaries, are ejected from the cluster after a few Gyr from formation. This follows in response to close single–binary interactions which harden the black hole binaries imparting large recoil velocities, and/or to binary coalescences via gravitational wave emission for which the induced recoil velocity can largely exceed the escape speed from the cluster (O’Leary et al. 2006; Downing et al. 2011). Either a single or a binary stellar black hole or no black hole is left at the centre after ejection of the bulk of the population.³

Davies et al. (2011; DMB11 hereafter) reconsider this channel of runaway merging of stellar black holes in dense star clusters in a broader context. They envisage the case of a galaxy undergoing a merger with another galaxy or the case of a large-scale gravitational instability in a galaxy which drives (in both cases) a major central inflow of gas on to a pre-existing NSC, i.e. an inflow that can even exceed the mass of the star cluster itself. In case the in-falling gas dominates the cluster gravitational potential, the dynamical behaviour of all stars in the cluster changes in response to the inevitable gas-induced increase of the dispersion velocity. Hard

² Note that in a follow up paper, Quinlan & Shapiro (1990) showed that in galactic nuclei there is the natural tendency of triggering at their centre runaway star–star collisions during the early stage of their evolution. The very massive star is then expected to collapse into a massive black hole. This channel was later re-proposed by Portegies Zwart & McMillan (2002) in the context of young and dense star clusters of lower mass after the recognition that a wide mass spectrum leads to rapid mass segregation and multiple stellar runaway collisions ending with the formation of a massive object of $100 M_{\odot}$.

³ There are theoretical claims that stellar mass black holes are present in some globular clusters (Moody & Sigurdsson 2009) and a recent observation seems to support this view (Strader et al. 2012).

¹ This pathway holds in enriched, yet metal-poor star clusters (those with metallicity below $\sim 10^{-3} Z_{\odot}$), as massive metal-enriched stars lose mass via intense wind during nuclear evolution leaving a lower mass black hole or a neutron star (Heger et al. 2003). Mergers of metal-rich stars can also be very disruptive (Glebbeek et al. 2009).

binaries present in the cluster (i.e. binaries which carry a binding energy per unit mass larger than the kinetic energy per unit mass of single stars) are turned nominally into soft binaries which soften when interacting with single stars. This process has the effect of reducing the dynamical heating of the cluster, now more susceptible to the gravothermal collapse. The cluster, dominated by the gravity of the underlying gas, may then enter a period of core collapse: stellar mass black holes in the hardest binaries start merging via gravitational radiation reaction before heating the cluster and/or being dynamically ejected. The enhanced escape speed due to the inflow reduces the effect of black hole ejection. Eventually, the black holes in the core merge in a runaway fashion. Central velocities as large as $\gtrsim 1000 \text{ km s}^{-1}$ need to be attained following a major gas inflow (see [DMB11](#)).

The details of this model, and in particular the effect of an inflow of gas on the fate of the stellar black holes, have not been exploited yet and future dedicated numerical experiments are necessary to assess the feasibility of this route. Hereon, we will assume that this channel operates in an NSC subjected to a major inflow, postponing to an incoming paper the analysis of the interaction of the gas with the stars and black holes in the cluster. As large central inflows of gas are expected to occur during the build-up of pre-galactic structures, this mechanism for black hole seed formation may be relevant during the early phases of galaxy formation.

The aim of this work is at exploring whether major inflows of gas occur at the centre of pre-galactic disc hosting an NSC, to assess the cosmological relevance of this process under the hypothesis that inflows of gas drive the runaway merger of the stellar black holes in these clusters. To this purpose, we study how a population of NSCs form and evolve inside dark matter haloes assembling out to redshifts as large as ~ 20 , in concordance with the Λ cold dark matter (Λ CDM) paradigm for hierarchical structure formation. To achieve this goal, we evolve ‘PINOCCHIO’ (Monaco, Theuns & Taffoni 2002), a code which follows the cosmological evolution of dark matter haloes with cosmic time, and a second code by [D09](#), [D10](#), [D12](#) which creates and follows the evolution of the baryonic components in the haloes, using physically motivated prescriptions for disc and SF in pre-galactic haloes. [D09](#), [D10](#), [D12](#) studied a scenario of black hole seed formation that jointly accounts for the early formation of a population of Pop III stars with their relic black holes, and at later times of young NSCs able to grow in their core a runaway star resulting from repeated stellar collisions which is fated to become a black hole of large mass. [D10](#) and [D12](#) select clusters having relaxation times shorter than the evolution time of the massive stars ($\lesssim 10^6 \text{ yr}$) for this to happen.

In this paper, we modify the code in order to include the Gas Induced black hole Runaway Merger model (hereon GIRM model) which is replacing the stellar-runaway NSC channel. The aim is at determining when black hole seeds form via the GIRM, tracing self-consistently the cosmological gas inflows in galactic haloes. This implies the selection of NSCs which undergo ordinary stellar evolution and are subject to major gas inflows during the cosmic assembly of structures. We note that the stellar-runaway NSC channel is complementary to the GIRM model as the latter evolves stars under ordinary conditions. Thus, a comparative analysis will enable us to assess the importance of GIRM, relative to Pop III and the stellar-runaway channel, in a cosmological context. In Section 2, we describe shortly the formation and assembly of dark matter haloes and their embedded NSCs, while in Section 3, we outline the input physics of the GIRM model, deferring the reader to [D10](#) and [D12](#) for details. Section 4 illustrates the results and Section 5 contains our conclusions.

2 DARK MATTER HALOES, GALACTIC DISCS AND THE FORMATION OF NSCS

‘PINOCCHIO’ is a code (Monaco et al. 2002) which evolves an initial density perturbation field, on a 3D grid, using the Lagrangian perturbation theory in order to generate catalogues of virialized haloes at different cosmic times, keeping track of the halo’s mass, position, velocity, spin parameter and merger history. In this paper, we evolve a cosmological volume of 10 Mpc in comoving length and adopt the Λ CDM cosmology with $\Omega_{\text{baryon}} = 0.041$, $\Omega_{\text{matter}} = 0.258$, $\Omega_{\Lambda} = 0.742$, $h = 0.742$, and $n_s = 0.963$ (Dunkley et al. 2009).

In this simulation, the mass resolution is of $M_{\text{h,min}} = 3 \times 10^5 M_{\odot}$ for the dark matter haloes, and is computed as the total mass in the box divided by the number of elements assigned at the onset of the simulation (Monaco et al. 2002). Dark matter elements lighter than $M_{\text{h,min}}$ do not form in the box. The corresponding resolution limit for baryons is of $5 \times 10^4 M_{\odot}$ but this limit does not represent the minimum mass scale of resolution within our semi-analytical treatment of NSC formation. According to theoretical studies, haloes with mass less than $M_{\text{h,min}}$ do not fulfil the conditions for SF and fragmentation at the redshifts explored (Tegmark et al. 1997; Barkana & Loeb 2001).

In our complex scheme (here simplified in its skeleton to outline only the key steps), virialized dark matter haloes, forming at any redshift, accrete baryonic gas in a fraction equal to $\Omega_{\text{baryon}}/\Omega_{\text{matter}}$. The gas, initially in virial equilibrium, cools down at a rate computed according to the available cooling channel (either molecular or atomic cooling depending on the metallicity of the gas in the halo) and condense into the centre of the halo. The code distinguishes between metal-free haloes (those with metallicity $Z < Z_{\text{crit}}$, where $Z_{\text{crit}} \sim 10^{-4.87} Z_{\odot}$ is the critical metallicity for fragmentation) and haloes enriched above Z_{crit} (Santoro & Shull 2006).

(i) In metal-free conditions, typical of the first collapsing haloes, the halo virial temperature is $T_{\text{vir}} < 10^4 \text{ K}$, and the only available cooling channel is that of molecular hydrogen (H_2). If enough H_2 is present in the halo, gas can cool down to $T \sim 200 \text{ K}$, reaching high enough densities to form a Pop III star. In the code, only a single Pop III star is allowed to form in haloes with $T_{\text{vir}} \gtrsim 10^3 \text{ K}$ (Tegmark et al. 1997) with a mass extracted from a top-heavy initial mass function extending from a minimum to a maximum mass of 10 and $300 M_{\odot}$, respectively ([D10](#)).

Pop III stars can produce a strong UV flux, able to affect the thermodynamics of gas inside the halo and in the neighbouring ones. In particular, the strong Lyman–Werner flux emitted is able to photodissociate H_2 molecules, thus quenching molecular cooling. Formation of new zero-metallicity stars is suppressed in those haloes in which the H_2 dissociation rate is higher than its formation rate. In massive haloes, above a threshold mass self-shielding of the gas, in the denser regions, can however prevent the disruption of molecular hydrogen (Machacek, Bryan & Abel 2001; Madau & Rees 2001) and this is accounted for in the simulation.⁴

(ii) In metal-enriched haloes (with typical virial temperatures $T_{\text{vir}} > 10^4$), gas cools down via both atomic and molecular cooling and collapses towards the halo centre. Assuming angular momentum conservation, the cool gas settles into a large-scale pre-galactic disc described as a rotationally supported self-gravitating Mestel

⁴ Note that in presence of a sufficiently high Lyman–Werner background, seed black holes can form via direct collapse of warm gas clouds in some haloes (Agarwal et al. 2012; Latif et al. 2013). This is a path which is not considered in this scheme.

disc. The disc keeps on growing in mass due to continuous infall of cool gas, and the progressive increase in the gas mass causes the disc to become Toomre unstable. Torques induced by self-gravity lead to a relatively fast redistribution of gas within the disc: the gas shocks and loses angular momentum thus sinking to the centre of the halo where it forms an inner disc. The inner disc develops a steeper profile than the outer unstable disc and will become the site of NSC formation. As gas flows in the inner disc, the surface density in the outer Mestel disc decreases until the Toomre parameter increases nearing the critical value for stability ($Q_{\text{crit}} \sim 2$, in the simulations considered). At this time, the central infall of gas stops. The overall process self-regulates to guarantee a condition of marginal stability in the outer disc. The mass routed in the central part and forming the inner disc then corresponds to the amount necessary for the outer disc to be marginally stable. The final configuration will then be characterized by an outer disc with Mestel profile and an inner disc with a steeper density profile (with surface density scaling as $R^{-5/3}$). The physical parameters of the two nested discs are then calculated self-consistently with the transition between the outer and inner discs occurring at a transition radius R_{tr} (D10).

This holds true if fragmentation of the gas, conducive to SF, does not take place overall in the outer disc. As reported in Lodato & Natarajan (2007), fragmentation occurs when the gravitationally induced stress into the disc is larger than a critical value. In the code, fragmentation is allowed where the cooling rate exceeds the adiabatic heating rate (D09). These two conditions determine the region where SF sets in, which can be defined introducing a characteristic radius R_{SF} . If the outer disc grows strongly unstable, widespread SF sets in consuming part of the gas that would otherwise flow into the inner disc. In this case $R_{\text{SF}} > R_{\text{tr}}$ and an NSC forms with a radius $R_{\text{cl}} = R_{\text{tr}}$ and a mass M_{cl} which is calculated self-consistently considering that left at disposal after gas consumption. By contrast, if the outer disc remains stable against fragmentation, SF is triggered in the inner disc, and an NSC forms with a radius corresponding to the SF radius, i.e. $R_{\text{cl}} = R_{\text{SF}}$ and a mass equal to the total mass of the inner disc turned into stars. A flow chart describing all the processes leading to the formation of an NSC, which has been described in this section, is reported in Fig. 1.

A parameter which determines the NSC mass, in the simulation, is η , controlling the extent of baryonic inflows from the outer to the inner disc. Since SF in the outer disc reduces the amount of gas that flows in, the net inflow rate, and thus the mass of the NSC at birth, is computed as the difference between the nominal inflow rate which an unstable outer disc would have and that consumed in stars. In our simulations, we assume η , as defined in D10, equal to 1. As shown in D10, the net inflow rate and the mass of the NSC at birth turn out to have a weak dependence on η (see fig. 2 of D10) since with increasing η more gas is consumed by extended SF before it can reach the inner disc. The total gas mass that has flown inwards, at the end of the simulation, turned out to be slightly lower for higher values of η . The continuous inflow of gas is a key ingredient for the model under study, as the NSC after birth is invaded by repeated episodes of gas accretion, thus leading to the evolution that we will explore in the incoming sections. Hereafter, we hypothesise that gas on to the NSC acts to deepen the potential well without turning into stars.

(iii) In our model, the physical consequences of SNe are included, for all channels, using motivated recipes, to account for gas depletion and metal pollution. Three million years after NSC formation, it is assumed that the most massive stars explode as SNe, primarily leading to gas evacuation at a rate correlated to the energy of the explosion. This affects the extent of gas inflows on the NSC at sub-

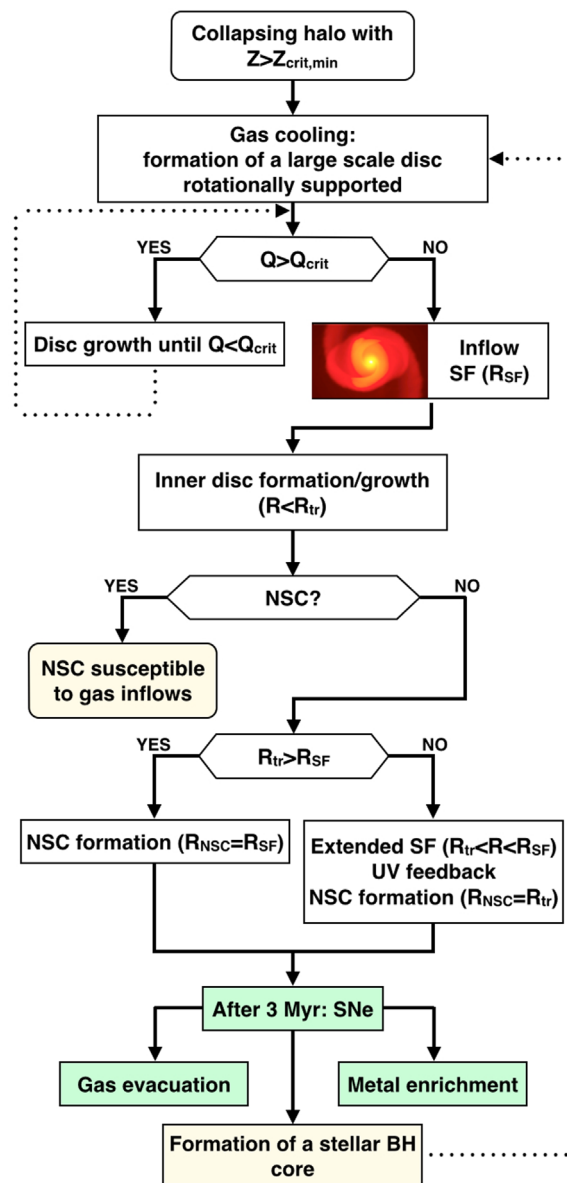


Figure 1. Flow chart of an isolated halo with $Z > Z_{\text{crit,min}}$, starting from gas cooling until the formation of an NSC in the centre of the halo. The processes/events in the flow chart are described in Section 3.

sequent times, as SF in the surroundings of the NSC is temporarily quenched. Similarly, metal pollution from SNe is accounted for using a simple parametric prescription which correlates the SNe rate with the rate of injection of metals. A fraction $f_{\text{metal}} = 1 - M_{\text{sh}}/M_{\text{sn}}$, with M_{sh} the gas mass removed from the halo (see DV10) and M_{sn} the total mass released by the SN, is then retained in the halo. We remark that in the explored range of metallicities, the masses of the NSC at birth turned out to depend weakly on the metal content (as shown in fig. 3 of D10).

The very massive stars in the NSC are assumed to leave behind a relic population of stellar mass black holes which form a core after mass segregating. In this paper, the core represents the site of formation of the seed black hole after the NSC has been subjected to repeated gas inflows.

(iv) In our cosmological scenario, haloes undergo mergers, and the merger history of any halo can be obtained from PINOCCHIO.

In the code, merger prescriptions read that: (a) the total, baryonic, stellar and metal masses of the new halo are computed as a sum of the masses of the two progenitors; (b) if the mass ratio between the haloes is less than 1/10, the spin parameter of the main progenitor is retained, otherwise a new value is computed following Bett et al. (2007); (c) the properties of the new pre-galactic disc are calculated taking into account the new mass and angular momentum, and then disc stability, eventual inflow and SF are re-evaluated; (d) if one or both the haloes host a seed black hole, different paths can be followed. In a major merger, the secondary black hole (if present) is able to reach the centre of the primary, while in a minor merger, it is left wandering in the new halo (Callegari et al. 2011). The code is able to describe the remnant at the end of the merger only, but it completely neglects all processes taking place during the merger events.

(v) NSCs start forming around redshift $z \sim 20$ when the Universe is 180 Myr old. With the code, we follow their evolution down to redshift $z \sim 6$ when the Universe is $\lesssim 1$ Gyr old. We then halt the simulations, since the code does not implement any accretion history important at lower redshifts (Merloni & Heinz 2013).

3 GAS INFLOWS ON TO NSCS

In this section, we first introduce the contraction parameter, describing the dynamical response of an NSC to an arbitrary inflow of gas, and later we illustrate the implementation of the new channel of black hole seed formation, in the cosmological simulation sketched in Section 2.

3.1 Contraction parameter

Consider the case of an NSC at the centre of a pre-galactic disc which is subjected to an inflow of gas, due to a perturbation inside the parent halo or due to a halo–halo merger, and let M_{gas} the total gas mass involved in the inflow. What is the kinematical response of the cluster to the inflow of gas? If, in the simplest hypothesis, the gas contributes only to the deepening of the potential well, this causes a change in the orbital velocity dispersion of the stars. Assuming that stars in the cluster move on nearly circular orbits and that their angular momentum is conserved during the inflow event, we have

$$l_* = m_* \sqrt{GM(< r_0)r_0} = m_* \sqrt{G(M(< r_0) + M_{\text{gas}})r}, \quad (1)$$

where r_0 and r are the stellar radii before and after the inflow event, respectively, and $M(< r_0)$ is the stellar mass within r_0 . In response to the inflow, the new radius is

$$r/r_0 = M(< r_0)/[M(< r_0) + M_{\text{gas}}]. \quad (2)$$

This is an oversimplifying assumption not only because stars do move on rosetta, eccentric orbits in star clusters but also because no assumption has been made on how the gas is distributed inside the star’s cluster, i.e. whether it is more clustered towards the centre or distributed over a much larger volume (assuming again for simplicity spherical symmetry).

In order to model different degrees of contraction for the cluster and redistribution of gas, we generalized this relation assuming a power law with a generic exponent ξ for the entire cluster, which can be written as

$$R_{\text{cl}}/R_{\text{cl},0} = [M_{\text{cl},0}/(M_{\text{cl},0} + M_{\text{gas}})]^\xi, \quad (3)$$

where R_{cl} and $R_{\text{cl},0}$ are the cluster radii before and after the inflow event, respectively. According to equation (3), $\xi = 1$.

The running value of the parameter ξ can be estimated more accurately, exploring as toy model a spherical inflow, of given mass M_{gas} , in a star cluster described by a Plummer potential of scale radius a_* initially. If during a spherical inflow, the angular momentum per unit mass of individual stars is conserved, then ξ varies between ~ 0 and ~ 3 , as illustrated in Fig. 2. This figure is obtained under the assumption that also the gas after the inflow settles into virial equilibrium following a Plummer profile with scale radius a_{gas} . In Fig. 2, we plot ξ as a function of a_{gas} for different values of the mass inflow M_{gas} . Varying a_{gas} is a way to mimic different cooling prescriptions for the gas which can contract down to a very small radius (in the absence of a modelling of the thermodynamical behaviour of the gas). As expected, the largest contraction occurs, for a given M_{gas} , in the limit of $a_{\text{gas}} \rightarrow 0$ and is larger the larger M_{gas} is. For a Plummer sphere, ξ saturates to a value equal to $\ln(2^{3/2}) = 2.8$ in the limit in which the whole mass M_{gas} has collapsed into a point.⁵

From this toy model, we notice that cluster contraction depends on how the gas concentrates within the cluster. Since the inflow of mass on the pre-existing star cluster can occur at any time according to the evolution of the halo’s cosmic environment, and can vary from episode to episode, the contraction parameter is very susceptible to conditions that allow for a wide range of values. To bracket uncertainties, we thus explore NSCs with inflows varying the contraction parameter ξ between a minimum value of 0.5 and a maximum of 3.

The contraction of the star cluster due to the gas inflows also leads to an increase of the velocity dispersion of the stars which is computed according to the virial theorem, once the new radius and new total cluster’s mass are known.

3.2 Modelling the gas-induced black hole runaway process in an NSC with inflows

Let $M_{\text{cl},0}$, $R_{\text{cl},0}$ and σ_{cl} be the mass, radius and 1D velocity dispersion of the star cluster at the time of its formation. Stellar mass black holes are assumed to form after the first three Myr and to mass seg-

⁵ The analytical estimates of ξ shown in Fig. 2 match well with those obtained by calculating the response of a star cluster to an external inflow, using a Monte Carlo integrator for the true dynamics of the stars (our stellar black holes) in a Plummer sphere (Galanti et al., in preparation).

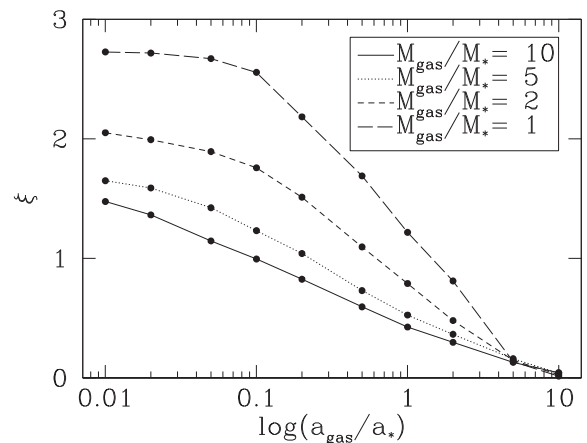


Figure 2. Contraction parameter ξ from equation (3) as a function of the ratio between the gas scale radius a_{gas} and the initial stellar scale radius a_* for different inflow masses.

regate shortly after within a core radius $R_{\text{BH-core},0} = 0.1R_{\text{cl},0}$. The typical mass segregation time-scale can be computed as

$$t_{\text{segr}} \approx \frac{\langle m_{\star} \rangle}{m_{\text{BH}}} \frac{N}{8 \log N} \frac{R_{\text{cl},0}}{v_{\star,0}}, \quad (4)$$

where $\langle m_{\star} \rangle$ is the mean stellar mass, m_{BH} the mean black hole mass, N the number of stars and black holes in the cluster and $v_{\star,0}$ is the stellar typical velocity which can be approximated with the 1D velocity dispersion $\sigma_{\text{cl},0}$ of the cluster. If we consider a typical NSC initial mass of $10^4 M_{\odot}$, with radius $R_{\text{cl},0} = 1$ pc, mean stellar mass of $\langle m_{\star} \rangle \simeq 1 M_{\odot}$ and $m_{\text{BH}} \sim 10 M_{\odot}$, the mass segregation time-scale is ~ 4 Myr. We thus assume that a core of stellar black holes forms 4 Myr after the NSC formation. We further define $M_{\text{BH-core},0}$ as the mass in stellar black holes present in the cluster core, and $\sigma_{\text{BH-core},0}$ the black hole velocity dispersion: we assume $M_{\text{BH-core},0} = 1.5 \times 10^{-3} M_{\text{cl},0}^6$ and $\sigma_{\text{BH-core},0} = 26\sigma_{\text{cl},0}$, where 26 corresponds to virial value $(GM_{\text{BH}}/R_{\text{BH-core},0})^{1/2}$.

Fig. 3 shows a schematic picture of the NSC contraction process driven by gas inflow, ending with the formation of the seed black holes. GIRM is implemented in the code as follows.

(i) Given a mass inflow M_{gas} on to the NSC, the radius R_{cl} is updated according to equation (3), where the exponent ξ is allowed to vary between 0.5 and 3, as explained in Section 3.1. The new velocity dispersion σ_{cl} is computed from the virial theorem, considering as mass the sum of the cluster and gas mass. Gas is allowed to settle into a disc of size R_{tr} , as a purely radial inflow would require an unphysical transport/cancellation of angular momentum. The gas disc has a surface density profile of the form $\Sigma_{\text{gas}} = \Sigma_0(R/R_{\text{tr}})^{-5/3}$ with $\Sigma_0 = M_{\text{gas}}/2\pi R_{\text{tr}}^2$.

⁶ This relation is derived from $M_{\text{core},0} = m_{\text{BH}}N_{\text{BH}}$, where $N_{\text{BH}} = \alpha N_{\star}$ with $\alpha = 0.0015$, and $M_{\text{cl},0} = \langle m_{\star} \rangle N_{\star} + m_{\text{BH}}N_{\text{BH}}$ (see DMB11).

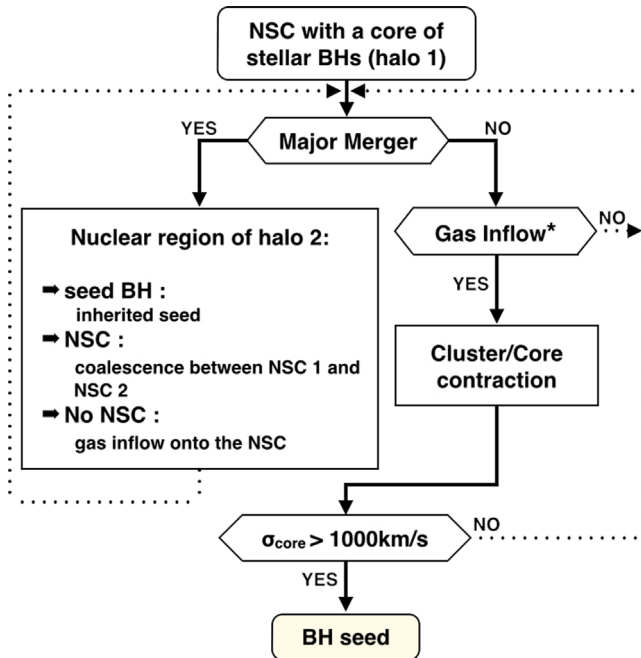


Figure 3. Flow chart reporting the NSC contraction process leading to the formation of a single seed BH from the merger among stellar mass black holes.

(ii) We compute the gas mass $M_{\text{gas,core}}$ enclosed in $R_{\text{BH-core}}$ from the above relation for the disc and update the stellar core radius $R_{\text{BH-core}}$ according to equation (3). The enhancement of the core velocity dispersion $\sigma_{\text{BH,core}}$ is computed from the virial relation using as mass the sum of $M_{\text{BH-core},0}$ and $M_{\text{gas,core}}$. If, in response to an inflow, $\sigma_{\text{BH-core}}$ exceeds 1000 km s^{-1} , we assume that the whole core of stellar black holes experiences GIRM, which leads to the formation of a seed of mass equal to $M_{\text{BH-core},0}$. The choice of 1000 km s^{-1} is motivated by the study of DMB11, representing the threshold for GIRM. In the DMB11 scenario, hard binaries coalesce before experiencing single-binary encounters and, at the same time, are retained in the core as the kicks from gravitational recoil are not large enough to allow black holes to escape from the cluster (having an escape speed $\sim 4000 \text{ km s}^{-1}$).

(iii) In presence of halo-halo mergers, NSCs are modelled using simple recipes which account for the additional inflows of gas (Mihos & Hernquist). In the case of major mergers (those with mass ratio larger than 1:10), we follow these prescriptions: (a) if only one halo hosts an NSC prior to the merger, the gas of the companion halo is added to the new halo causing an inflow in the first, and the cluster and core parameters are updated considering a rapid infall. The new radius and mass of the star cluster with its embedded black hole are computed using the contraction law; (b) if both haloes hosted an NSC, we merged the two into a single new cluster, and update the cluster properties following the prescriptions in Ciotti, Lanzoni & Volonteri (2007). Assuming that during the merger no mass is lost, energy conservation allows us to estimate the virial radius R_{12} of the new cluster core of black holes as

$$\frac{1}{R_{12}} = \left(\frac{M_{\text{BH},1} + M_{\text{g},1}}{M_{\text{BH},12} + M_{\text{g},12}} \right)^2 \frac{1}{R_1} + \left(\frac{M_{\text{BH},2} + M_{\text{g},2}}{M_{\text{BH},12} + M_{\text{g},12}} \right)^2 \frac{1}{R_2}, \quad (5)$$

where $M_{\text{BH},1}$ and $M_{\text{BH},2}$ are the masses of the black hole cores of the progenitor clusters, $M_{\text{g},1}$ and $M_{\text{g},2}$ the gas masses in the cores, $M_{\text{BH},12}$ and $M_{\text{g},12}$ the total mass in black holes and gas of the new star clusters, respectively and R_1 and R_2 are the virial radii of the progenitor clusters; (c) if one halo had already a seed black hole with a mass above $260 M_{\odot}$ relic of a Pop III star, this black hole is incorporated in the resulting halo as a new seed; (d) if both haloes hosted a seed black hole, we assumed the instantaneous coalescence of the two black holes into a more massive seed.

(iv) In the case of minor mergers, NSCs are modelled assuming that the only change in their properties is due to an additional gas inflow. Black holes and clusters from the smaller halo are left wandering in the outer region of the resulting galaxy, and are not allowed to sink into the nuclear region (Callegari et al. 2011).

(v) We further explored, as ancillary study, NSCs with velocity dispersions in the interval between 40 and 100 km s^{-1} . These NSCs have no relation with the GIRM scenario, but their presence can be easily tracked, within the cosmological scheme explored here. Their relatively high-velocity dispersion (between 40 and 100 km s^{-1}) can be natal or more likely is acquired following a gas inflow. The request on the velocity enhancement here is less severe than in GIRM. This will enable us to investigate on the likelihood of an alternative scenario by Miller & Davies (2012). In this new context, NSCs with velocities dispersions in this selected range can grow a black hole seed from a stellar mass black hole (or binary black hole). Stellar mass holes, relic of massive stars, have two possible fates in these NSCs: they are either all ejected or a single (or binary) remains. The black hole (binary) which avoided ejection, can later grow via tidal captures. Dynamical arguments by Miller & Davies (2012) seem to support this picture. We thus aim to calculate the number of NSCs with velocity dispersion between 40 and 100 km s^{-1} , resulting

either from the direct collapse of an unstable disc, or after a phase of gas inflow into a pre-existing cluster.

4 RESULTS

4.1 Seed black holes from GIRM in NSCs

We ran a suite of simulations, for three different values of $\xi = 0.5, 1$ and 3 for the contraction parameter. The cosmological box explored has a size of 10 Mpc and has been evolved from redshift $z \sim 40$ down to redshift $z \sim 6$, to test if the GIRM channel is able to produce a population of seed black holes large enough to explain the most massive black holes found in the Universe at redshift up to ~ 7 . We halt integration at $z \sim 6$ as our code does not include any process of accretion that can become important below this redshift.

In the simulations, we considered the Pop III and GIRM channels. They are expected to contribute to the early generations of seed black holes at different cosmic epochs, as the formation of NSCs in pre-galactic discs (a necessary condition for the GIRM to operate) requires some degree of metal pollution of the intergalactic medium from the explosions of the massive Pop III stars. We remark that the GIRM channel does not pose any constraint on the level of metallicity of the parent halo, and hence on the time of formation, provided Pop III stars have enhanced the metallicity above a threshold $Z_{\text{crit}} \sim 10^{-4.87} Z_{\odot}$ (see D10 and D12). The GIRM path requires the formation of ordinary star clusters and thus a population of stellar mass black holes from the core collapse of the massive stars.

Figs 4 and 5 show the number of haloes relative to the total $f_{\text{BH}} = N_{\text{BH}, z} / N_{\text{halo}, z}$ which host a newly formed black hole at any given redshift.⁷ The simulation resolution reported in the plots is computed as $1/N_{\text{haloes}, z}$.

There exists an earlier epoch of black hole seed formation from Pop III, around $z \sim 20$, and a second, from the GIRM channel around $z \sim 8, 10$ and 15 according to the values of ξ (as given in Table 1), with an overlap with the Pop III channel for $\xi = 3$. A more rapid contraction of the star cluster in response to the gas inflows

⁷ The case for $\xi = 1$ is intermediate between Figs 4 and 5 and is not reported for the sake of simplicity.

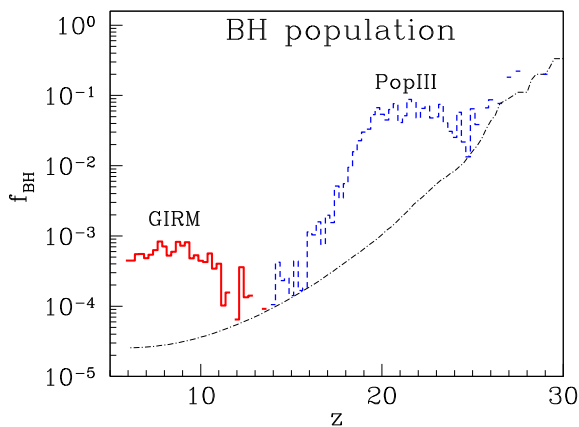


Figure 4. Fraction f_{BH} of haloes hosting a newly formed seed black hole as a function of redshift, from redshift $z = 30$ down to $z = 6$. The blue line refers to the Pop III channel; the red solid line refers to the fraction of black holes with mass above $260 M_{\odot}$ resulting from the GIRM channel, for a contraction parameter $\xi = 0.5$. The black dash-dotted line is the simulation resolution.

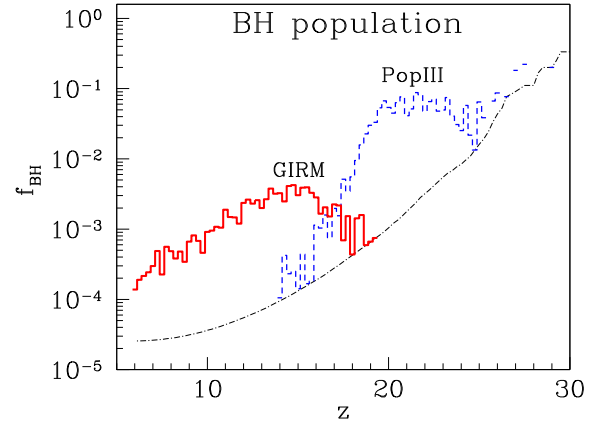


Figure 5. Fraction f_{BH} of haloes hosting a newly formed seed black hole as a function of redshift, from redshift $z = 30$ down to $z = 6$. The blue line refers to the Pop III channel; the red solid line refers to the fraction of black holes with mass above $260 M_{\odot}$ resulting from the GIRM channel for a contraction parameter $\xi = 3$. The black dash-dotted line is the simulation resolution.

Table 1. The number of black hole seeds formed from the GIRM channel (upper panel) and from Pop III (lower panel); the mean black hole seed mass and the redshift where their formation peaks, considering the three adopted values of ξ .

ξ	#seed	$\langle M/M_{\odot} \rangle$	z_{peak}
0.5	405	1301.1	7.75
1.0	637	1173.4	10.0
3.0	1054	987.5	14.75
PopIII	822	70.5	27.5

(i.e. for $\xi = 3$) makes black hole formation to occur earlier and to produce a larger number of seeds. Later, the observed decline mirrors the bottom-up hierarchical build-up of the haloes and of their embedded star clusters: less massive haloes form first and require lower gas inflows to produce a seed, while heavier haloes require a greater amount of gas and are less in number. In the case of $\xi = 0.5$, black hole seed formation occurs at later epochs as there is the need of a larger inflow of gas to trigger the collapse of the black hole star clusters. The decline in the Pop III channel is instead due to metal pollution from the first Pop III stars which quenches the formation of black hole seeds from pristine gas. Table 1 shows that the number of black hole seeds in the cosmological box increases with increasing ξ , and that the channel is competitive to that from Pop III. The fraction f_{BH} is larger for the Pop III channel, but with cosmic time, the absolute number of sufficiently massive dark matter haloes increases so that the absolute number of natal black hole haloes is larger as z decreases. The evolution of the relative contribution to the black hole seed population due to Pop III and GIRM channels is depicted in Fig. 6, where we report the total seed comoving mass density as a function of redshift. In the plot, the different lines correspond to the Pop III channel and GIRM channels for different values of ξ . In addition, also the total seed comoving mass density has been represented.

As in D10, black hole seeds from Pop III stars have a typical small mass ($\sim 70 M_{\odot}$), while seeds from the GIRM channel have a larger mass, of about $\gtrsim 1000 M_{\odot}$, as the entire cluster of stellar black

holes is assumed to undergo runaway merger, after a major inflow of gas. The mean mass of black holes formed via the GIRM channel decreases with increasing ξ and this can be explained with the larger fraction of NSCs with smaller masses able to core collapse before $z = 6$. In general, to form a seed the required inflow of gas is at least comparable with the mass of the target star cluster.

Fig. 7 shows the black hole seed mass distribution, for the GIRM channel, for the three values of ξ : 0.5, 1 and 3. As already mentioned, the number of black hole seeds increases with increasing ξ . Despite the different mean mass, the peak of the mass distribution is around the same value of $350 M_{\odot}$, mirroring the shape of the mass distribution of the parent NSCs housing the seeds, depicted in Fig. 8. The mass of the parent cluster is measured prior to the mass inflow that led to the core collapse.

In addition, Figs 9 and 10 give the total mass of the inflow (due to repeated accretion events) within the transition radius R_{tr} as a function of the black hole seed mass, evaluated when the velocity dispersion in the core reaches $\sigma \gtrsim 1000 \text{ km s}^{-1}$. The red lines represent the best fit obtained assuming that $M_{\text{gas}} \propto M_{\text{BH}}$. When

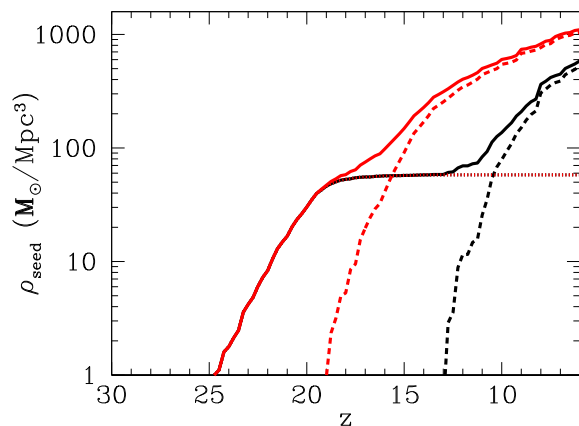


Figure 6. Black hole mass density versus redshift for the two channels. The dotted line refers to the Pop III path. The dashed lines refer to the GIRM channel for $\xi = 0.5$ (right) and 3 (left). The total seed mass densities are plotted with the solid lines, for $\xi = 0.5$ (right) and $\xi = 3$ (left).

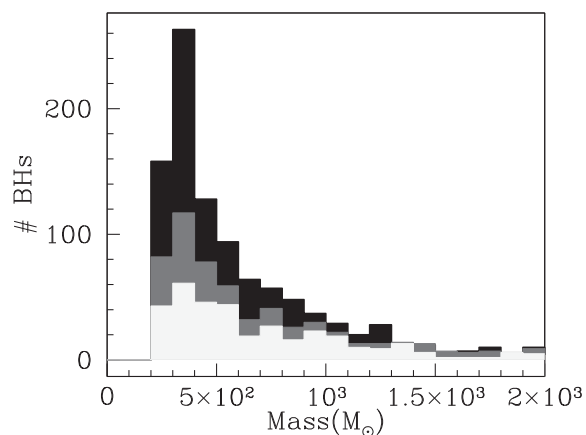


Figure 7. Mass distribution of seed black holes formed via the GIRM channel, for $\xi = 0.5, 1$ and 3. The black histogram corresponds to $\xi = 3$, grey to $\xi = 1$ and beige to $\xi = 0.5$. Black hole seeds have a typical mass of about $350 M_{\odot}$, while the mean mass depends on the ξ , and is given in Table 1.

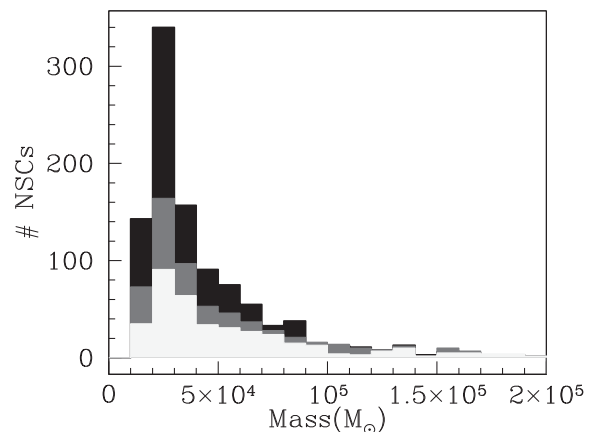


Figure 8. Mass distribution of the NSCs hosting seed black holes formed via the GIRM channel, for $\xi = 0.5, 1$ and 3. The black histogram corresponds to $\xi = 3$, grey to $\xi = 1$ and beige to $\xi = 0.5$. The largest fraction of NSCs have a typical mass, prior to the gas inflow, of about $3.5 \times 10^4 M_{\odot}$.

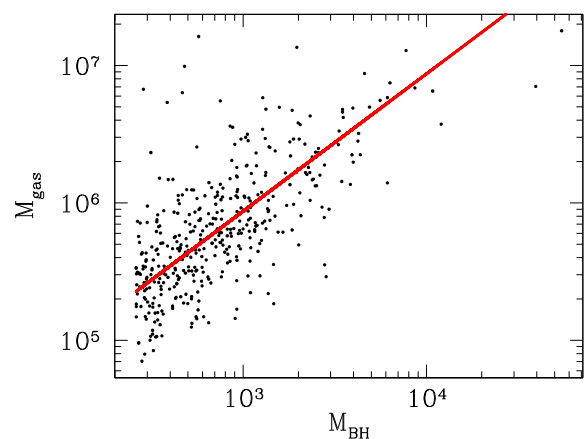


Figure 9. Gas mass resulting from inflows as a function of the seed black hole mass for the GIRM channel with $\xi = 0.5$. The red solid line corresponds to the linear fit obtained assuming a zero black hole mass for $M_{\text{gas}} = 0$.

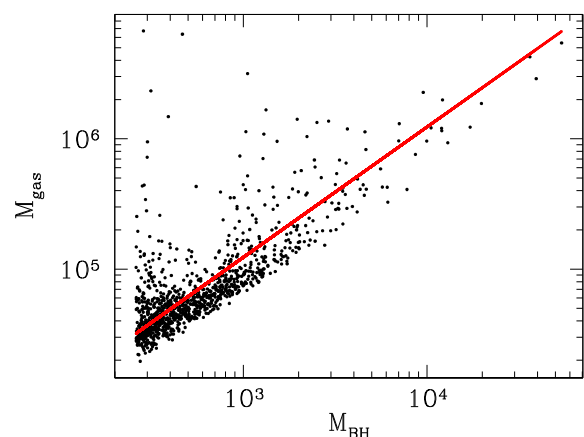


Figure 10. Gas mass resulting from inflows as a function of the seed black hole mass for the GIRM channel with $\xi = 3$. The red solid line corresponds to the linear fit obtained as in Fig. 9.

$\xi = 0.5$, the best line gives $M_{\text{gas}} \simeq 123M_{\text{BH}}$, while for $\xi = 3$, we obtained $M_{\text{gas}} \simeq 870M_{\text{BH}}$. These results show that the total inflow needed to drive the NSC core to $\sigma \gtrsim 1000 \text{ km s}^{-1}$ varies from a minimum corresponding to roughly the NSC mass up to values as large as 10–50 times the NSC mass.

As the extent of a gas inflow is related to the halo gas fraction and to mergers, we also expect a correlation between the total inflow needed for the GIRM to occur and the host halo mass. Combining these two relations, we find that the ratio between the gas inflow mass and the seed black hole mass is almost independent of the host halo mass, as reported in Figs 11 and 12. In the case of $\xi = 0.5$, only the most massive haloes ($> 3 \times 10^8 M_{\odot}$) can host a seed black hole from GIRM, while for a more efficient contraction ($\xi = 3$), seeds are hosted also in less massive haloes. At very large halo masses, the ratio varies also of two orders of magnitude, and the largest values are probably due to haloes with very large inflows, overcoming the necessary threshold for GIRM to occur.

Moreover, we find that the occupation fraction of black holes F_{BH} (formed via both Pop III and GIRM channels) is a function of redshift, and it strongly depends on the host halo mass. Figs 13

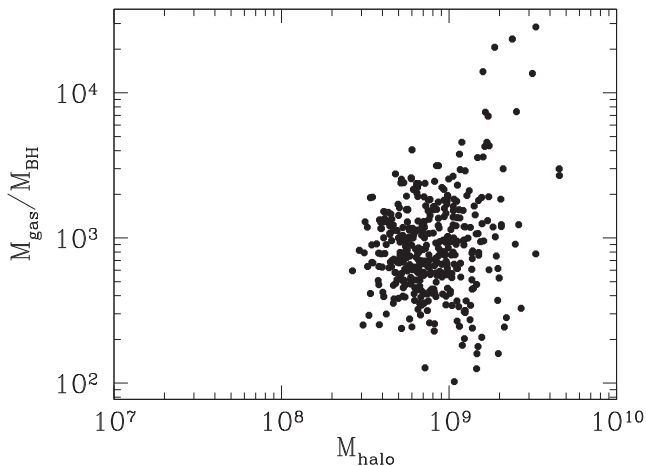


Figure 11. Gas mass to seed black hole mass ratio resulting from inflows as a function of the host halo mass for the GIRM channel with $\xi = 0.5$. The ratio is almost independent of the host halo mass, with the exception of the very large ones (where the inflow could be quite larger than that needed to GIRM) and it is almost constant with a value with an order of 10^3 .

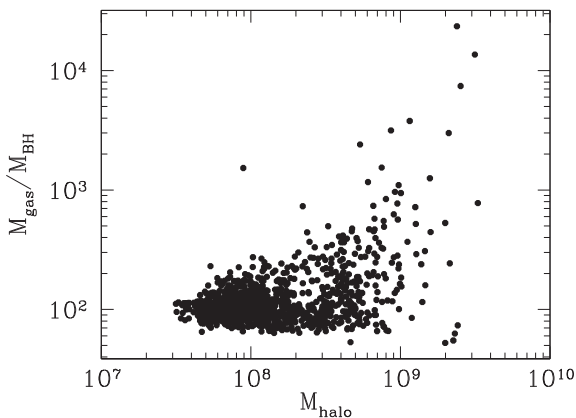


Figure 12. Gas mass to seed black hole mass ratio resulting from inflows as a function of the host halo mass for the GIRM channel with $\xi = 3$. Also in this case the ratio weakly depends on the host halo mass, except for the very large ones (same as in Fig. 11).

and 14 show that at redshift $z = 6$ haloes with masses larger than $8\text{--}9 \times 10^9 M_{\odot}$ host a black hole, and haloes with masses lower than $2 \times 10^8 M_{\odot}$ do not at all. Note also the weak dependence on ξ of F_{BH} . For higher redshift, all the lines shift to lower masses, according to our cosmological model.

4.2 Stellar black holes in NSCs

As anticipated in Section 2, NSCs with velocity dispersions in the interval $40\text{--}100 \text{ km s}^{-1}$ may be able to retain a black hole or a binary black hole of stellar mass, as suggested in Miller & Davies (2012). These clusters have gravitational potential wells deep enough, and two-body relaxation times short enough for mass segregation to lead to formation of a core of stellar black holes. Having these cluster's high escape speeds, black hole ejection by three-body encounters or gravitational wave recoil is incomplete and either a single stellar black hole or a black hole binary remains in the cluster which may later grow by capturing stars. Here, we briefly touch upon this model, by counting, in this sub-section, the number of NSCs forming inside the pre-galactic discs that have their velocity dispersion

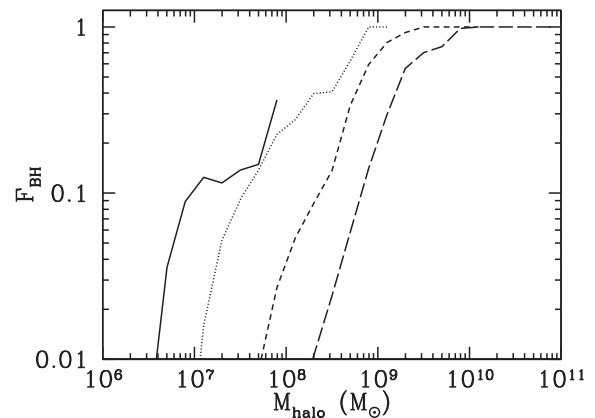


Figure 13. Occupation fraction of seed black holes versus halo mass assuming $\xi = 0.5$. From left to right, the lines show values at redshift $z = 20, 15, 10$ and 6 , respectively.

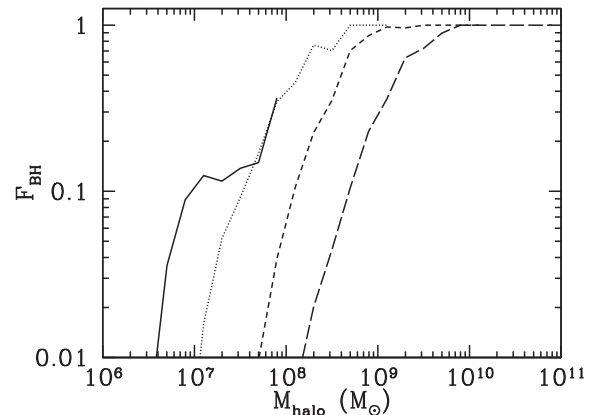


Figure 14. Occupation fraction of seed black holes versus halo mass assuming $\xi = 3$. From left to right, the lines show values at redshift $z = 20, 15, 10$ and 6 , respectively.

Table 2. The number of NSC candidates for core collapse following a gas inflow or a merger, leaving a single stellar mass black hole after ejection of the black holes in the core, as discussed in Section 6, for the three different values of ξ .

ξ	$\max\{\#\text{seed}\}$	$\langle M_{\text{cl}}/M_{\odot} \rangle$
0.5	4003	5.83×10^4
1.0	4421	5.22×10^4
3.0	4814	4.90×10^4

above 40 km s^{-1} , or rise it due to a cosmological mass inflow or a merger. The results are given in Table 2 and can be considered as an upper limit to the stellar black hole population retained in these systems. The calculation indicates that at the centres of pre-galactic discs there might be the conditions to build star clusters in which an intermediate-mass black hole of stellar origin can form, and this could be a further channel of formation of seeds. From a comparison between Table 1 and Table 2, we note that the number of NSCs where this scenario may happen is 4–10 higher than in the standard GIRM.

5 CONCLUSIONS

In this paper, we explored the formation of black hole seeds of $\lesssim 10^3 M_{\odot}$, resulting from the dynamical collapse of stellar black holes in NSCs undergoing major gas inflows, at the centre of pre-galactic discs forming at very high redshifts.

We explored the properties of this population of forming seeds combining the clustering of dark matter haloes extracted from ‘PINOCCHIO’ with a semi-analytical model which incorporates the physics of the inflows in a simplified form. Inflows on to the central star clusters are triggered either by instabilities in the evolving pre-galactic disc and/or from mergers. Our aim was at comparing the efficiency of the GIRM channel with the already-explored channels from Pop III (here reported as a reference) and from the collapse of supra-massive stars in young dense star clusters.

Our channel is active around redshift $z \sim 10\text{--}15$ as soon as the first NSCs form in the dark matter haloes. Contrary to the two channels mentioned above, the GIRM is insensitive to the metallicity of the environment. The GIRM, by hypothesis, can occur in any star cluster that formed a core of ordinary stellar black holes, provided that (i) the star cluster is subjected to a massive inflow of gas which rises the central dispersion velocity above a given threshold, and (ii) the stellar black holes present in the core had no time to be ejected by single–binary encounters prior the massive inflow. The lapse time between inflow events at the redshifts explored is $\lesssim 0.1$ Gyr. Black hole ejection in star clusters are seen to occur typically on times longer than ~ 1 Gyr (Downing et al. 2011), so that at early cosmic epochs this effect can be neglected. Conservatively, the results can be considered as upper limits.

We find that the GIRM channel is competitive, when compared to the channels studied in D09, D10 and D12 and can occur in concomitance with the formation of seeds from other channels, and in particular with that from runaway collisions of stars, in young dense clusters for which there is a partial overlap in the redshift space. We halt the simulation at $z \sim 6$, as our model do not account for the black hole growth due to accretion. Typically, the black holes have seed masses in excess of $300 M_{\odot}$ with a mean of $\sim 1000 M_{\odot}$,

opening the possibility that these black holes may later grow as supermassive at redshifts as early as $z \sim 7$, typical of the most distant quasars.

These masses are in the range of the so-called intermediate-mass black holes, which have not been yet observed in the Universe. If these black holes do not remain confined in galaxy centres but become wandering (like in the case of minor mergers of the host halo with a larger one), they could reach $z = 0$ without becoming massive black holes, and they could become potentially observable with their original mass.

There is no model yet that can describe the thermodynamics of a massive inflow of gas on to a pre-existing star cluster. The gas funnelled towards the centre of the cluster likely cools and fragment into stars, forming a more massive nuclear cluster nested into a primitive, lighter one. The key requirement of the DMB11 model, not proved to be realistic yet, is a steepening of the gravitational potential such as to lead to a major enhancement of the velocity dispersion inside the core of stellar mass black holes to trigger their relativistic collapse. Further modelling is necessary in this direction (Galanti et al., in preparation).

ACKNOWLEDGEMENTS

The authors are pleased to thank Jillian Bellovary, Melvin Davies and Coleman Miller for a critical reading of the manuscript and their enlightening comments, and the referee whose comments and queries helped improving the manuscript. MC and MV thank the Kavli Institute for Theoretical Physics at UC Santa Barbara for hospitality during progress on this work, while the programme ‘A Universe of Black Holes’ was taking place. MV acknowledges funding support from a Marie Curie Career Integration grant (PCIG10-GA-2011-303609) within the framework FP7/PEOPLE/2012/CIG. This research was supported in part by the National Science Foundation under grant no. NSF PHY11-25915, through the Kavli Institute for Theoretical Physics and its programme ‘A Universe of Black Holes’.

REFERENCES

- Abel T., Bryan G. L., Norman M. L., 2002, *Science*, 295, 93
 Agarwal B., Khochfar S., Johnson J. L., Neistein E., Dalla Vecchia C., Livio M., 2012, *MNRAS*, 425, 2854
 Barkana R., Loeb A., 2001, *Phys. Rep.*, 349, 125
 Begelman M. C., 2010, *MNRAS*, 402, 673
 Begelman M. C., Volonteri M., Rees M. J., 2006, *MNRAS*, 370, 289
 Begelman M. C., Rossi E. M., Armitage P. J., 2008, *MNRAS*, 387, 1649
 Bett P., Eke V., Frenk C. S., Jenkins A., Helly J., Navarro J., 2007, *MNRAS*, 376, 215
 Bromm V., Loeb A., 2003, *ApJ*, 596, 34
 Bromm V., Coppi P. S., Larson R. B., 2002, *ApJ*, 564, 23
 Callegari S., Kazantzidis S., Mayer L., Colpi M., Bellovary J. M., Quinn T., Wadsley J., 2011, *ApJ*, 729, 85
 Choi J.-H., Shlosman I., Begelman M. C., 2013, *ApJ*, 774, 149
 Ciotti L., Lanzoni B., Volonteri M., 2007, *ApJ*, 658, 65
 Clark P. C., Glover S. C. O., Klessen R. S., Bromm V., 2011, *ApJ*, 727, 110
 Davies M. B., Miller M. C., Bellovary J. M., 2011, *ApJ*, 740, L42 (DMB11)
 Devecchi B., Volonteri M., 2009, *ApJ*, 694, 302 (D09)
 Devecchi B., Volonteri M., Colpi M., Haardt F., 2010, *MNRAS*, 409, 1057 (D10)
 Devecchi B., Volonteri M., Rossi E. M., Colpi M., Portegies Zwart S., 2012, *MNRAS*, 421, 1465 (D12)
 Di Matteo T., Colberg J., Springel V., Hernquist L., Sijacki D., 2008, *ApJ*, 676, 33
 Dotan C., Rossi E. M., Shaviv N. J., 2011, *MNRAS*, 417, 3035

- Downing J. M. B., Benacquista M. J., Giersz M., Spurzem R., 2011, *MNRAS*, 416, 133
- Dunkley J. et al., 2009, *ApJS*, 180, 306
- Ferrara A., Haardt F., Salvaterra R., 2013, *MNRAS*, 434, 2600
- Glebbeeck E., Gaburov E., de Mink S. E., Pols O. R., Portegies Zwart S. F., 2009, *A&A*, 497, 255
- Greif T. H., Springel V., White S. D. M., Glover S. C. O., Clark P. C., Smith R. J., Klessen R. S., Bromm V., 2011, *ApJ*, 737, 75
- Gürkan M. A., Freitag M., Rasio F. A., 2004, *ApJ*, 604, 632
- Haiman Z., Thoul A. A., Loeb A., 1996, *ApJ*, 464, 523
- Heger A., Fryer C. L., Woosley S. E., Langer N., Hartmann D. H., 2003, *ApJ*, 591, 288
- Koushiappas S. M., Bullock J. S., Dekel A., 2004, *MNRAS*, 354, 292
- Latif M. A., Schleicher D. R. G., Schmidt W., Niemeyer J. C., 2013, *MNRAS*, 436, 2989
- Lodato G., Natarajan P., 2006, *MNRAS*, 371, 1813
- Lodato G., Natarajan P., 2007, *MNRAS*, 377, L64
- Machacek M. E., Bryan G. L., Abel T., 2001, *ApJ*, 548, 509
- Madau P., Rees M. J., 2001, *ApJ*, 551, L27
- Mayer L., Kazantzidis S., Escala A., Callegari S., 2010, *Nature*, 466, 1082
- Merloni A., Heinz S., 2013, in Oswalt T. D., Keel W. C., eds, *Planets, Stars and Stellar Systems, Vol. 6: Evolution of Active Galactic Nuclei*. Springer-Verlag, Berlin, p. 503
- Mihos J. C., Hernquist L., 1996, *ApJ*, 464, 641
- Miller M. C., Davies M. B., 2012, *ApJ*, 755, 81
- Monaco P., Theuns T., Taffoni G., 2002, *MNRAS*, 331, 587
- Montero P. J., Janka H.-T., Müller E., 2012, *ApJ*, 749, 37
- Moody K., Sigurdsson S., 2009, *ApJ*, 690, 1370
- Mortlock D. J. et al., 2011, *Nature*, 474, 616
- O’Leary R. M., Rasio F. A., Fregeau J. M., Ivanova N., O’Shaughnessy R., 2006, *ApJ*, 637, 937
- Omukai K., Palla F., 2001, *ApJ*, 561, L55
- Portegies Zwart S. F., McMillan S. L. W., 2002, *ApJ*, 576, 899
- Quinlan G. D., Shapiro S. L., 1987, *ApJ*, 321, 199
- Quinlan G. D., Shapiro S. L., 1989, *ApJ*, 343, 725
- Quinlan G. D., Shapiro S. L., 1990, *ApJ*, 356, 483
- Santoro F., Shull J. M., 2006, *ApJ*, 643, 26
- Schleicher D. R. G., Palla F., Ferrara A., Galli D., Latif M., 2013, *A&A*, 558, A59
- Strader J., Chomiuk L., Maccarone T. J., Miller-Jones J. C. A., Seth A. C., 2012, *Nature*, 490, 71
- Tegmark M., Silk J., Rees M. J., Blanchard A., Abel T., Palla F., 1997, *ApJ*, 474, 1
- Volonteri M., 2010, *A&AR*, 18, 279
- Wise J. H., Turk M. J., Norman M. L., Abel T., 2012, *ApJ*, 745, 50
- Yoshida N., Omukai K., Hernquist L., 2008, *Science*, 321, 669

This paper has been typeset from a $\text{\TeX}/\text{\LaTeX}$ file prepared by the author.